

# **The deubiquitinase Usp8 regulates $\alpha$ -synuclein clearance and modifies its toxicity in Lewy body disease.**

Alexopoulou Z.<sup>1</sup>, Lang J.D.<sup>1\*</sup>, Perrett R.M.<sup>1\*</sup> Elschami M.<sup>1</sup>,  
Hurry M.<sup>1</sup>, Kim H.T.<sup>2</sup>, Mazaraki D.<sup>1</sup>, Szabo A.<sup>3</sup>, Kessler BM<sup>4</sup>, Goldberg A.L.<sup>2</sup>,  
Ansorge O.<sup>1</sup>, Fulga T.A.<sup>3</sup>, Tofaris G.K.<sup>1</sup>

\*These authors contributed equally

<sup>1</sup> Nuffield Department of Clinical Neuroscience, University of Oxford, UK

<sup>2</sup>Department of Cell Biology, Harvard Medical School, Boston, USA

<sup>3</sup> Weatherall Institute of Molecular Medicine, Radcliffe Department of Medicine  
University of Oxford, UK

<sup>4</sup>Target Discovery Institute, Nuffield Department of Medicine, University of  
Oxford, UK

**Correspondence:** George K. Tofaris

Nuffield Department of Clinical Neurosciences

University of Oxford, John Radcliffe Hospital, Oxford, OX3 9DU, UK

Email: george.tofaris@ndcn.ox.ac.uk

Tel: 0044(0) 1865 231858

Fax: 0044(0) 1865 234699

**Classification:** Biological Sciences/Neuroscience

**Key Words:** Ubiquitin, Parkinson's disease, endosome

In Parkinson's disease, misfolded  $\alpha$ -synuclein accumulates, often in a ubiquitinated form, in neuronal inclusions termed Lewy bodies. An important outstanding question is whether ubiquitination in Lewy bodies is directly relevant to  $\alpha$ -synuclein trafficking or turnover and Parkinson's pathogenesis. By comparative analysis in human post-mortem brains, we found that ubiquitin immunoreactivity in Lewy bodies is largely due to K63-linked ubiquitin chains and markedly reduced in the substantia nigra compared to the neocortex. ~~The ubiquitin~~ staining in cells with Lewy bodies inversely correlated with the content and pathological localization of the deubiquitinase Usp8. Usp8 interacted and partly co-localized with  $\alpha$ -synuclein in endosomal membranes and both in cells and after purification, it deubiquitinated K63-linked chains on  $\alpha$ -synuclein. Knockdown of Usp8 in the *Drosophila* eye reduced  $\alpha$ -synuclein levels and  $\alpha$ -synuclein-induced eye toxicity. Accordingly, in human cells Usp8 knockdown increased the lysosomal degradation of  $\alpha$ -synuclein. In the dopaminergic neurons of the *Drosophila* model, unlike knockdown of other deubiquitinases, Usp8 protected from  $\alpha$ -synuclein-induced locomotor deficits and cell loss. These findings strongly suggest that removal of K63-linked ubiquitin chains on  $\alpha$ -synuclein by Usp8 is a critical mechanism that reduces its lysosomal degradation in dopaminergic neurons and may contribute to  $\alpha$ -synuclein accumulation in Lewy body disease.

**Significance** A cardinal feature of Parkinson's disease pathology is the aggregation of  $\alpha$ -synuclein in ubiquitin-positive inclusions termed Lewy

bodies. Yet the composition of ubiquitin conjugates in these inclusions and their role in  $\alpha$ -synuclein pathobiology remains unclear. Here we demonstrate that  $\alpha$ -synuclein inclusions contain K63-linked ubiquitin chains, which are strikingly reduced in the dopaminergic neurons. In these neurons, the deubiquitinase Usp8 is present in Lewy bodies, and its content related inversely with the extent of K63-linked ubiquitination. Our mechanistic studies *in vitro* and in flies indicate that Usp8 interacts with and deconjugates K63-linked ubiquitin chains on  $\alpha$ -synuclein, prolonging its half-life and increasing its toxicity. Thus, Usp8 appears to be a critical factor determining  $\alpha$ -synuclein levels that could be targeted for therapies.

## **Lewy**

Parkinson's disease (PD) is the second most common neurodegenerative disorder and is characterized pathologically by neuronal death and the formation of intracellular inclusions termed Lewy bodies (LB). Although primarily a movement disorder with predilection for the pigmented neurons of the substantia nigra (SN), these neuropathological features are eventually widespread affecting other areas of the brain, especially the entorhinal and anterior cingulate cortex (1). Misfolded  $\alpha$ -synuclein is the major constituent of LB (2) and the density of cortical LB correlates with the extent of cognitive dysfunction (3). In familial cases, patients with a triplication of the  *$\alpha$ -synuclein* gene develop dementia at an earlier age than those with duplications (4), whereas in sporadic LB disease, soluble  $\alpha$ -synuclein oligomers are increased in patients with dementia in the absence of changes in  *$\alpha$ -synuclein* transcription (5). These findings strongly suggest that the

neuronal level of  $\alpha$ -synuclein is critical in determining the development of diffuse neurodegeneration with LB. Conversely, differential expression or activation of enzymes that regulate  $\alpha$ -synuclein levels may partly explain the neuronal vulnerability and regional progression of  $\alpha$ -synuclein pathology.

Most cellular proteins are selectively targeted for degradation by conjugation to a ubiquitin chain. This modification involves activation of ubiquitin by the enzyme, E1, transfer of the reactive ubiquitin to a ubiquitin-conjugating enzyme (E2), and then conjugation by a ubiquitin ligase (E3) to a protein substrate or a preceding ubiquitin to form a ubiquitin chain. Ubiquitin contains seven lysine residues, each of which can be linked to the C-terminus of another ubiquitin molecule through an isopeptide bond. While formation of ubiquitin chains in which the ubiquitins are covalently linked through their K48 or K11 residues leads to the degradation of cytosolic proteins by 26S proteasomes, attachment of chains linked through K63 residues to membrane-associated proteins targets them for lysosomal degradation. Both these ubiquitin-dependent degradative processes, as well as macroautophagy, contribute to clearance of  $\alpha$ -synuclein (6, 7). For example, in the endosomal process, the ubiquitin ligase Nedd4 forms K63-linked chains on  $\alpha$ -synuclein to target it to lysosomes (7). At the proteasome and during endosomal uptake, ubiquitin chains are disassembled by deubiquitinating enzymes (DUBs) so that the ubiquitin molecules can be reused in subsequent rounds of degradation, but this action of DUBs can also serve to prevent the degradation of substrates.

Ubiquitin immunoreactivity is a robust neuropathological hallmark of LB (8, 9) and a fraction of  $\alpha$ -synuclein in LB is ubiquitinated (10, 11). Therefore,



enzymes that catalyze ubiquitin conjugation or deubiquitination may contribute to the cell's response to  $\alpha$ -synuclein accumulation. However, the composition of ubiquitin chains in LB in different regions of the brain remains unknown. As a consequence, it has been widely assumed that ubiquitin immunoreactivity is a non-specific modification or a surrogate marker of impaired proteasomal function in PD and other  $\alpha$ -synucleinopathies (12). In this study we revisited this assertion and investigated regional differences in LB ubiquitination, explored its enzymatic basis and significance for  $\alpha$ -synuclein-induced toxicity.

## Results

**Ubiquitination of LB involves K63-linked ubiquitin chains and is regionally distinct:** Although it has long been known that LB can be stained with antibodies against ubiquitin (8, 9), the molecular underpinnings of this modification remain unknown. To address this issue, we performed a comprehensive investigation of the pattern and composition of ubiquitin conjugates in these inclusions across different brain regions using twenty cases of almost pure  $\alpha$ -synuclein pathology that were identified in the Thomas Willis Brain Collection (University of Oxford). The cases were characterized in terms of neuropathological staging (1) and LB numbers as shown in **Suppl. Table 1**. Using serial sections, we then quantified the percentage of ubiquitin positive inclusions relative to  $\alpha$ -synuclein immunoreactivity in three brain regions (**Fig. 1 A-C**), where at least eight LB were detected (SN, range: 10-119; anterior cingulate, AC, range: 8-249; entorhinal cortex, EC, range: 11-258). In the cortex a high proportion of the inclusions were positive with a pan-ubiquitin antibody with similar percentages detected in the two regions that

were examined: AC 69.2% ( $\pm$  5.3%) and EC 62.2% ( $\pm$  4.5%). Unexpectedly, the percentage of LB that were ubiquitin-positive was lower in the SN (27.3%  $\pm$  3.2%,  $p < 0.0001^*$ ,  $n = 14$  One-Way ANOVA, **Fig. 1 C and D**). The low percentage of ubiquitin-positive inclusions in the SN was detected irrespective of the pathological stage or clinical diagnosis and this fraction was even lower in incidental LB cases than in LB disease (**Fig. 1 E**), suggesting that ubiquitin immunoreactivity is not related to the extent of cell death in this region. To investigate whether ubiquitin chains that target proteins for degradation are present in LB, we used linkage-specific ubiquitin antibodies against Lys-63 and Lys-48. We found only occasional staining of inclusions with anti-K48 ubiquitin antibodies regardless of the epitope retrieval method. In striking contrast, anti-K63 ubiquitin antibodies showed extensive immunoreactivity both in the cortex and SN (**Fig. 1 A**). To confirm that K63-specific antibodies stain the pathological inclusions, we used double labeling immunofluorescence confocal microscopy and found strong co-localization of the K63-specific and the  $\alpha$ -synuclein antibodies (**Fig. 1 B**). Quantitative analysis revealed that in the cortex, the percentage of K63-linked ubiquitin immunoreactive inclusions was much higher (AC 49.0%  $\pm$  4.7% and EC 52.5%  $\pm$  6.0%), than in the SN (12.8%  $\pm$  2.4%;  $p < 0.0001^*$ ,  $n = 14$ , Wilcoxon-Mann-Whitney/Kruskal-Wallis test, **Fig. 1 D**). A similar pattern was seen with the pan-ubiquitin antibody and there was a highly significant positive correlation between K63-specific and pan-ubiquitin immunoreactive inclusions ( $\rho = 0.4990$ ;  $p < 0.0004^*$  Spearman's rho, **Suppl Fig. 1 A**). It should be noted that another, less well recognized inclusion in the SN of patients with PD, the intranuclear Marinesco body, was universally positive with K63-specific

antibodies (**Suppl Fig. 1 C**), indicating that the regional pattern of LB staining is not due to technical differences in antibody binding between the cortex and SN. Finally, we tested and confirmed the specificity of these antibodies by immunoblotting against single lysine ubiquitin chains as shown in **Suppl Fig. 2**. Thus, ubiquitin conjugates in LB as assessed by immunohistochemistry, are to a large extent K63-specific chains with a regionally distinct pattern between the SN and cortex.

**K63-linked ubiquitin conjugates in LB inversely correlate with pathological localization of Usp8:** Inside cells, K63-linked ubiquitin conjugates function in cell signaling, DNA repair, and in trafficking proteins to the endosomal or autophagic pathways. The Endosomal Sorting Complex Required for Transport (ESCRT) components STAM1/2 and HRS help deliver proteins bearing K63-linked chains to the endosomal pathway (13, 14) and in this process, two DUBs, Usp8 and AMSH disassemble the ubiquitin chain to release ubiquitin (15-19). Distinct ubiquitin-binding proteins, such as p62 and NRB1, can serve as specific adaptations that promote autophagic degradation of ubiquitinated protein aggregates and organelles (20). We therefore investigated whether differences in the levels of such interactors in the substantia nigra and cortex of the same brain or in these regions of healthy and disease brains could explain the differences in ubiquitin immunoreactivity (**Suppl Fig. 3**). Quantitative immunoblotting revealed a significant increase in Usp8 levels in brain lysates of patients with LB disease compared to healthy controls in the SN ( $p=0.0028^*$ , Wilcoxon-Mann-Whitney/Krusal-Wallis test, **Fig. 2 A-C**), but not in the cortex. This biochemical finding was corroborated

by the detection of a substantial localization of Usp8 but not AMSH in neurons with pathological inclusions (**Fig. 2 D-F**). Double labeling immunofluorescence confocal microscopy confirmed that Usp8 was co-localized with the  $\alpha$ -synuclein-positive inclusions (**Fig. 2 G**). Importantly, quantitative analysis of Usp8 immunoreactivity showed a striking inverse correlation with either pan-ubiquitin or K63-specific ubiquitin staining: while only a low number of cortical inclusions stained with Usp8 antibodies (AC 14.7% $\pm$ 4.0%; EC 16.8% $\pm$ 2.8%), many more inclusions were Usp8 positive in the SN (43.9% $\pm$ 5.0%;  $p < 0.0001^*$   $n=14$ ; Wilcoxon-Mann-Whitney/Kruskal-Wallis test, **Fig. 2 H**; negative correlation coefficient  $\rho = -0.5044$ ,  $p < 0.0002^*$ ;  $\rho = -0.4186$ ,  $p = 0.0038^*$ , Spearman's rho, **Fig. 2 I-J**). It is noteworthy that the soluble levels of LC3II and p62, two widely used markers of autophagic degradation did not differ between cases versus controls or between regions (**Suppl Fig. 3**). Thus, contrary to the prevailing views, our data suggest that ubiquitin immunoreactivity in Lewy body disease may represent regional differences in protein deubiquitination and that Usp8 may be the critical determinant of this pattern and therefore important in the pathogenesis of sporadic PD.

**Usp8 interacts with and co-localizes with  $\alpha$ -synuclein in neurons:** Usp8 has pleiotropic effects in the regulation of endosomal trafficking: it directly deubiquitinates endosomal cargo proteins (15-19), but it is also implicated in the stability of the ESCRT complexes (21, 22). Because  $\alpha$ -synuclein is the most abundant protein in LB, one possible explanation for our observations in post-mortem brains is that the co-localisation of Usp8 with  $\alpha$ -synuclein in LB may signify a direct interaction between them. To address this question, we first

co-transfected FLAG-tagged wild-type Usp8 or catalytically inactive (Cys786 to Ala) Usp8<sup>CA</sup> or an empty vector and untagged human  $\alpha$ -synuclein in HEK-293T cells. When overexpressed,  $\alpha$ -synuclein was immunoprecipitated from lysates of cells expressing wild-type or catalytically inactive Usp8 with anti-FLAG tagged antibodies but not from lysates of control expressing an empty vector (**Fig. 3 A**). To test the possibility that monomeric or toxic forms of  $\alpha$ -synuclein may bind to and inhibit the activity of Usp8, we assayed for such an effect by using a HA-tagged ubiquitin-bromide (HA-Ub-Br<sub>2</sub>) probe, which can conjugate to the catalytic cysteine of most DUBs and thus can be used to measure their activity. The amount of HA-Ub-modified Usp8 was not altered by the overexpression of wild-type or PD-related mutant forms of  $\alpha$ -synuclein and did not correlate with increasing  $\alpha$ -synuclein levels in HEK-293T cells (**Fig. 3 B**). To investigate whether the interaction between Usp8 and  $\alpha$ -synuclein may be of physiological relevance, we asked whether they co-localize on endosomal membranes, a known site of action for Usp8. We first confirmed in HEK-293T cells, that although Usp8 was primarily cytosolic, it co-localized to a small extent with early but not late or recycling endosomes using either endogenous or transfected (Rab 5, Rab7, Rab11) markers (**Suppl Fig. 5**), in accordance with previous studies that reported a transient association of Usp8 with early sorting endosomes in HeLa cells (15). To investigate whether Usp8 interacts with  $\alpha$ -synuclein at specific endosomal compartments, we used bimolecular fluorescence complementation signifying Usp8/ $\alpha$ -synuclein interaction (green) with expression of endosomal Rabs (Rab5, Rab7, Rab11) tagged to a Red fluorescent protein and assessed the extent of co-localisation (yellow). This analysis showed that although the

interaction of Usp8 and  $\alpha$ -synuclein was detected in the cytosol, puncta of increased signal intensity co-localised principally with Rab5 rather than Rab7 or Rab11 positive endosomes (**Fig. 3 C**). To investigate the normal neuronal localization of these proteins we asked whether endogenous Usp8 and  $\alpha$ -synuclein co-localize in induced pluripotent stem cell (iPSc)-derived human dopaminergic neurons. We first tested and confirmed that these cells express both neuronal ( $\beta$ -III tubulin) and dopaminergic (tyrosine hydroxylase, TH and G protein-activated inward rectifier potassium channel 2, GIRK2) markers (**Suppl Fig. 4**). In these neurons, we found that Usp8 is detected in cytosolic puncta, which partly co-localized with  $\alpha$ -synuclein and overlapped to some degree with markers of the early sorting (anti-EEA1) but not the late (anti-LBPA) endosome (**Fig. 3 D**). Collectively, our data demonstrate that  $\alpha$ -synuclein directly interacts and co-localizes with Usp8 in cells, including human iPSc-derived dopaminergic neurons, and suggest that this interaction may involve at least transiently association with primarily early (Rab5-positive) endosomes.

**Usp8 de-ubiquitinates  $\alpha$ -synuclein in human cells:** To assess whether  $\alpha$ -synuclein is a substrate of Usp8, we transiently transfected HA-tagged ubiquitin in HEK-293T. The overexpressed wild-type but not catalytically inactive Usp8 caused a marked decrease in the content of ubiquitinated endogenous  $\alpha$ -synuclein in HEK-293T cells as shown by HA pull-down and staining with two different anti- $\alpha$ -synuclein antibodies (Syn1, **Fig 4 A** and C20, **Suppl Fig. 6 B**). In addition, by expressing HA-tagged single lysine ubiquitin, which is capable of only forming K63 or K48 linkages,

we found that in human cells overexpression of wild-type Usp8 de-conjugated chains containing both K63- and K48-linkages on  $\alpha$ -synuclein but showed preference for K63-linked ubiquitin chains (**Fig. 4 B**). It is noteworthy that on the same immunoblots, total ubiquitination of immunoprecipitated substrates was similar across all the experimental conditions, suggesting that the activity of Usp8 is selective against certain substrates. To further investigate the site of the Usp8/ $\alpha$ -synuclein interaction, we generated a deletion mutant of Usp8 lacking the Microtubule Interacting and Transport (MIT) domain, which was previously shown to mediate its endosomal association (21). Expression of this construct reduced but did not abolish the ability of Usp8 to de-ubiquitinate  $\alpha$ -synuclein in HEK-293T cells (**Fig. 4 C**). In addition, expression of the related DUB Usp7 had less activity against  $\alpha$ -synuclein when compared to Usp8 (**Fig. 4 C**). Thus, regional differences in LB ubiquitination may be explained, at least partly, by differences in their content of Usp8, which deubiquitinates  $\alpha$ -synuclein.

To further assess this model, we reconstituted the deubiquitination of  $\alpha$ -synuclein *in vitro*. Building on our prior finding that the ubiquitin ligase Nedd4 forms K63-linked ubiquitin chains on  $\alpha$ -synuclein (7), we compared the abilities of seven diverse cysteine protease DUBs at equimolar concentrations, (OTUB1, OTUB2, JosD2, Usp2, Usp5, Usp7 and Usp8) to digest K63-linked ubiquitin chains on  $\alpha$ -synuclein. Although all seven DUBs were active *in vitro* as evidenced by their binding to HA-ubiquitin-bromide, only Usp8, and the closely related enzyme Usp7, could hydrolyze the K63-linked chains on  $\alpha$ -synuclein (**Fig. 4D and Suppl. Fig 7**).

## **Deubiquitination by Usp8 regulates $\alpha$ -synuclein degradation by the**

**lysosome:** Deubiquitination by Usp8 was previously reported either to slow the degradation of substrates and promote their recycling (16-19) or facilitate endosomal trafficking and lysosomal degradation (21, 22). Because Usp8 is up-regulated in neurons with LB pathology, we tested the effect of increased Usp8 expression on  $\alpha$ -synuclein clearance in the presence of cycloheximide to prevent protein synthesis. Overexpression of Usp8 in HEK-293T cells, reduced the rate of clearance of endogenous  $\alpha$ -synuclein (**Fig. 5 A**) without causing an enlargement of early endosomes (**Suppl Fig. 5 D**), as had been reported in some cell lines (15). To test if these findings on the function of Usp8 on  $\alpha$ -synuclein degradation were restricted to these non-neuronal cells or caused only by DUB overexpression, we generated and validated lentiviral particles expressing shRNA against Usp8 in SH-SY5Y neuroblastoma cells, a cell line that expresses dopaminergic markers. Upon transduction, this construct markedly reduced the levels of Usp8 in SH-SY5Y. Strikingly, knockdown of Usp8 reduced endogenous  $\alpha$ -synuclein levels by approximately 35% (**Fig. 5 B**,  $p=0.0031$ ,  $n=5$ ) and increased the amount of immunoprecipitated ubiquitinated  $\alpha$ -synuclein (**Fig. 5 C**). The prediction of these experiments is that  $\alpha$ -synuclein trafficking to and degradation by the lysosomal pathway is increased when Usp8 is knocked down. To investigate this model, we treated SH-SY5Y cells lacking Usp8 or Scr shRNA controls with chloroquine (50 $\mu$ M) or lactacystin (5 $\mu$ M) for 8h and measured the level of  $\alpha$ -synuclein in membrane fractions that are enriched in endosomal and lysosomal compartments. We found that at baseline the level of  $\alpha$ -synuclein in this fraction was significantly reduced when Usp8 is knocked down as



expected from our data in total lysates and increased within 8 h of treatment with chloroquine but not lactacystin (**Fig. 5 C**). These data indicate that blocking the lysosome but not the proteasome increases  $\alpha$ -synuclein in cells lacking Usp8, suggesting that they exhibit accelerated lysosomal degradation of  $\alpha$ -synuclein.

**Usp8 knockdown rescues  $\alpha$ -synuclein-induced toxicity in the *Drosophila* model:** Our neuropathological and cell-based studies suggest that in  $\alpha$ -synucleinopathies, increased deubiquitination by Usp8 in nigral neurons may be harmful, at least partly by increasing  $\alpha$ -synuclein levels. We tested this prediction by expressing  $\alpha$ -synuclein in the fly eye, which has proven to be a valuable experimental model of  $\alpha$ -synuclein-induced toxicity (23, 24). This assay showed that the rough eye phenotype caused by ectopic expression of either human wild-type  $\alpha$ -synuclein or the A53T mutant  $\alpha$ -synuclein was prevented by concomitant knockdown of Usp8 (**Fig. 6 A, B**). In this model, the levels of  $\alpha$ -synuclein mRNA measured by qPCR was not lower in single than in double transgenic flies thus excluding a phenotype due to GAL4 dilution in double transgenic flies (**Fig. 6 A, B**). In control experiments, we showed that the rough eye phenotype was not observed with *GMR*-GAL4 driver alone (**Fig. 6 C**). In addition, we showed that the eye phenotype was not improved when A53T  $\alpha$ -synuclein was co-expressed with RNAi against the other endosomal DUB AMSH (**Fig. 6 C**), the proteasomal DUB Usp14 or Usp47 (**Suppl Fig 8 A**). In addition, the wild-type  $\alpha$ -synuclein phenotype was worsened when co-expressed with an RNAi against the ESCRT I protein Vps28, a downstream interactor in Usp8-mediated endosomal trafficking (**Fig. 6 C**). Importantly, we also showed that the rough eye phenotype caused by

two pathogenic proteins, expanded Ataxin 3 (**Fig. 6 D**) and expanded huntingtin (**Suppl Fig 8 B**), was not rescued by Usp8 knockdown. We confirmed the functional efficiency of Usp8 knockdown by detecting the previously documented wing defect (17) when the RNAi was expressed under the *MS1096*-GAL4 driver (**Suppl. Fig. 8 C**).

To assess the relevance of our finding in SH-SY5Y cells that endogenous Usp8 knockdown reduces  $\alpha$ -synuclein levels (**Fig. 5 B**) in the *Drosophila* model using an alternative RNAi approach, we performed serial fractionation of fly head lysates and measured the intensity of the monomeric  $\alpha$ -synuclein band as a ratio to actin loading control in the cytosolic and pelleted fractions of single and double transgenic flies. When Usp8 was knocked down, wild-type or A53T  $\alpha$ -synuclein protein level was reduced (**Fig. 6 E**) even though  $\alpha$ -synuclein mRNA levels were unchanged (**Fig 6 A, B**).

Finally, to corroborate our findings in the eye using an alternative readout of toxicity and to investigate whether similar mechanisms function in the dopaminergic neurons, we knocked down Usp8 specifically in these neurons of the *Drosophila* model of  $\alpha$ -synuclein toxicity using the dopamine decarboxylase, *ddc*-GAL4 driver. Strikingly, we found that knockdown of Usp8, but not knockdown of AMSH or JosD2, prevented the age-dependent locomotor defect caused by expression of the human A53T mutant  $\alpha$ -synuclein in dopaminergic neurons (**Fig. 6 F**). Interestingly, Usp8 knockdown in dopaminergic cells reduced the loss of the PPM1/2 cluster of dopaminergic

neurons (**Fig. 6 G**) that is most vulnerable in the *Drosophila*  $\alpha$ -synuclein model (23-25) and typically correlates with the locomotor deficit.

## Discussion

Although the presence of ubiquitin has long been recognized as a characteristic feature of LB, the origins and nature of the LB-associated ubiquitin conjugates have been unclear. The present data indicate that ubiquitination in these inclusions is comprised primarily of K63-linked conjugates and is regionally distinct. These findings challenge the long-held view that ubiquitin immunoreactivity represents a non-specific modification or the end product of impaired proteasome function. A targeted screen for potential interactors involved in the shuttling of K63-linked chains revealed up-regulation and pathological localization of the DUB Usp8, whose content correlated inversely with the extent of LB ubiquitination in diseased brains. To our knowledge, this dramatic pathological staining pattern identifies Usp8 as one of the best LB surrogates in pigmented neurons. Accordingly, transcriptomic analysis in immunolaser captured, microdissected nigral neurons showed up-regulation of Usp8 mRNA in neurons with LB (26). Collectively, these data in human pathological specimens, firmly establish Usp8 as a critical factor in the pathogenesis of sporadic PD and suggest an important role for K63-linked polyubiquitin chains in  $\alpha$ -synuclein degradation. It is noteworthy that K63-linked ubiquitin chains were detected in about half of the ubiquitin-immunoreactive LB, suggesting that additional linkages, other than K48-linked chains that we excluded, may be present. However, based on a number of previous studies by us and others that identified primarily

monoubiquitinated  $\alpha$ -synuclein in LB extracts by immunoblotting (10, 11, 27), it is most likely that the remaining immunoreactivity represents singly or multiply mono-ubiquitinated  $\alpha$ -synuclein, which could be the end-product of a deubiquitination reaction.

Usp8 shows some selectivity for recombinant K63 ubiquitin linkages *in vitro* (28, 29). However, when compared with other DUBs of the cysteine protease type, Usp8 as well as of the closely related enzyme Usp7, showed strong capacity to hydrolyse K63-linked ubiquitinated on  $\alpha$ -synuclein *in vitro*. In yeast, the Usp8 ortholog, Doa4 is an essential DUB for the maintenance of the free ubiquitin pool upon which endosomal trafficking is specifically dependent (30, 31). In mammalian cells, Usp8 regulates the recycling of membrane-associated proteins in a process that involves K63-linked substrate ubiquitination (16-19). Thus, normally in cells K63-linked ubiquitin chains are continually being hydrolyzed by Usp8, which serves an important function in endosomal-lysosomal trafficking. We and others have previously shown that the ubiquitin ligase Nedd4 and its yeast ortholog Rsp5 conjugate K63-linked chains on  $\alpha$ -synuclein, promoting its trafficking by the endosomal route (7, 32, 33) and  $\alpha$ -synuclein is enriched in endosomal compartments (34, 35). At the synapse, Nedd4 is responsible for formation of K63-linked chains that is antagonized by Usp8 (36) and *in vitro* these enzymes have opposing activities on  $\alpha$ -synuclein ubiquitination. Because  $\alpha$ -synuclein functions in the synaptic vesicle release by transient association with membranes (37), it is likely that these enzymes are critical in the regulation of its physiological function in brain. Although further work is needed to understand the molecular basis of this regulation, the close proximity of Usp8 to endosomes suggests

that its function on  $\alpha$ -synuclein turnover may involve reversible endosomal localization as shown for other substrates (15-19). Accordingly in cells, Usp8 and  $\alpha$ -synuclein interaction occurs at least partly in endosomes and deconjugation of preferentially K63-linked ubiquitin chains on  $\alpha$ -synuclein is enhanced by the N-terminal MIT domain of Usp8 that mediates its endosomal anchoring (21), whereas knockdown of Usp8 accelerates the degradation of  $\alpha$ -synuclein by lysosomes. K63-linked ubiquitin chains also mediate the autophagic degradation of aggregated proteins (13) and their presence in LB may also signify an attempt to clear misfolded  $\alpha$ -synuclein after its aggregation. It is likely that Usp8 is important in both the trafficking of normal as well as misfolded  $\alpha$ -synuclein, opposing its clearance by either an endosomal- or autophagic-lysosomal route respectively. For example, the Nedd4 ortholog in yeast Rsp5, which functions in endosomal trafficking, also regulates ubiquitin-mediated autophagy (38) and aggregated  $\alpha$ -synuclein is also ubiquitinated by Nedd4 *in vitro* (24). Whether additional DUBs such as Usp7 serve a direct role in  $\alpha$ -synuclein pathobiology requires further investigation.

Why Usp8 is induced in neurons with LB and whether this is a maladaptive response to enhance recycling of ubiquitin or other substrates is unclear. It is noteworthy that both *in vivo* and in cultured cells, Usp8 knockdown reduced total  $\alpha$ -synuclein content, even though  $\alpha$ -synuclein is degraded by multiple pathways (6, 7, 39). Consequently, impaired processing of  $\alpha$ -synuclein by Usp8 could contribute to its pathological accumulation in LB and the buildup of K63-linked ubiquitin chains. As indicated by hereditary cases with  $\alpha$ -synuclein multiplications, a small increase of less than 1.5-fold in

$\alpha$ -synuclein protein levels is sufficient to cause neurodegeneration with LB (4). It is thus possible that in disease, induction of Usp8 in neurons with LB promotes the accumulation and toxicity of  $\alpha$ -synuclein. This conclusion is strongly supported by our findings in flies, that Usp8 knockdown, but not knockdown of other DUBs, protected against different readouts of  $\alpha$ -synuclein toxicity (i.e. rough eye phenotype, locomotor defects and cell loss) at least partly by reducing  $\alpha$ -synuclein levels. Interestingly, Usp8 expression in the normal mouse brain is higher in neurons of the compact compared to those in the reticulate part of the substantia nigra (40). Given that Usp8 slows the degradation of  $\alpha$ -synuclein, this differential expression may account at least in part for the selective vulnerability of the compact region of the substantia nigra to  $\alpha$ -synuclein accumulation and neurodegeneration.

In summary, we have shown that ubiquitin immunoreactivity in LB is comprised of K63-linked ubiquitin chains, is regionally distinct and identified the DUB Usp8 as one potentially critical regulator of this pattern. Collectively, our biochemical and *in vivo* studies suggest that one mechanism by which up-regulation of Usp8 could contribute to PD pathogenesis is by opposing the clearance of  $\alpha$ -synuclein. Thus, although Usp8 serves some essential functions, in  $\alpha$ -synucleinopathies it may be a potential therapeutic target for small molecule inhibitors.

## **Materials and Methods**

**Staining of human brain sections:** Brain tissue from 20 patients (4 ILB, 5 PD, 11 PDD/LBD) was obtained from the brain bank of the John Radcliffe Hospital in Oxford (Suppl. Table 1). Tissue was formalin fixed and paraffin-

embedded, and serially sectioned at 7  $\mu\text{m}$  with a sliding microtome. Staining was performed using the Histostain-Plus detection kit (Life Technologies, Paisley, UK) and the HISTAR detection kit STAR3000C (AbD Serotec, Oxford, UK) as detailed in the *SI Appendix*. Lewy body pathology was assessed according to the recommendations of the third report of the Dementia with Lewy Bodies Consortium (41) and also by Braak stage (1). For fluorescence double labeling, following dewaxation and rehydration sections underwent epitope retrieval and preincubation with 10% goat serum at room temperature for 1 h before incubation with primary antibodies overnight at 4°C. For double-immunofluorescence Alexa Fluor® secondary antibodies (1:500, Life Technologies) at 488nm (green), 568nm (red) and 594nm (far red) were used. Autofluorescent background was blocked by sudan black and sections were mounted using fluorescence mounting medium (Dako, Cambridge, UK) containing 1 $\mu\text{g/ml}$  DAPI (Sigma).

**Immunoprecipitation:** Cell lysate supernatants were incubated overnight at 4°C with anti-HA or anti-FLAG antibodies (Sigma) or 2F12 anti- $\alpha$ -synuclein antibodies. Equilibrated Protein G Sepharose beads (P3926, Sigma) were then added for further 2 h at 4°C. The beads were washed three times with TBS-T, resuspended in 1x NuPAGE® LDS sample buffer with NuPAGE® Sample Reducing Agent (Life Technologies) and heated at 95°C for 10 min before loading onto the gel.

**Immunoblotting:** Brain samples were homogenized in ice-cold lysis buffer (50 mM Tris-HCl [pH 7.4], 150 mM sodium chloride, 1% NP-40, 0.1% SDS,

1mM PMSF; 1mM N-ethylmaleimide, all from Sigma) and centrifuged for 10min at 15,000g at 4°C. For fractionation of SH-SY5Y, the cells were resuspended in buffer (150mM NaCl, 10mM Tris pH 7.4 with complete protease inhibitor cocktail, 1mM PMSF and 1mM N-ethylmaleimide) and syringed with 25 gauge needle 10 times on ice followed by brief vortexing and the process was repeated three times with 2 min intervals on ice. Lysates were spun down at 600g for 10 min to remove debris and the supernatants were centrifuged at 100,000g for 1 h. The supernatant was designated as the cytosolic fraction and the pellet was resuspended in lysis buffer containing detergents (150mM NaCl, 10mM Tris pH 7.4 with complete protease inhibitor cocktail, 1mM PMSF, 1mM N-ethylmaleimide, 1%NP-40, 0.1% SDS) and centrifuged at 100,000g for 30 min. The supernatant was designated the membranous fraction. The protein content of the resulting supernatants was measured using the BCA assay (Thermo Fisher Scientific, Cramlington, UK). Equal amounts of protein were mixed with NuPAGE® Tris-Acetate SDS Running Buffer (Life Technologies) containing NuPAGE® Sample Reducing Agent (Life Technologies) and heated at 95°C for 10 min before separated on 4-12% SDS-PAGE gels (NuPAGE Novex Bis-Tris Gels, Life Technologies) and electrotransferred onto a nitrocellulose membrane (Amersham Protran 0.45, GE Healthcare, Buckingham, UK) in transfer buffer (25 mM Tris, 192 mM glycine, 20% (v/v) methanol). After blocking with 4% nonfat powdered milk in PBS containing 0.1% Tween- 20 (Sigma) for 1 h, primary antibodies were incubated with the membrane overnight at 4°C and binding was visualized after washing with peroxidase labeled anti-rabbit or anti-mouse secondary antibodies (GE Healthcare; 1:10000) and enhanced



chemiluminescence (GE Healthcare). Relative quantitation of the protein of interest to loading control was measured using ImageJ.

**Cell Culture and Transfection:** BE(2)-M17 cells(called M17D; ATCC number CRL-2267) stably expressing  $\alpha$ -synuclein, HEK293T cells and SH-SY5Y cells, which express  $\alpha$ -synuclein endogenously were maintained at 37°C and 5% CO<sub>2</sub> in DMEM containing 10% (v/v) fetal calf serum (Sigma) and 1% (v/v) penicillin/streptomycin/amphotericin-b (Life Technologies). Cells were grown to 60-80% confluency and transfected with plasmid DNA using Lipofectamine 2000. Plasmids used and mutagenesis is described in detailed in the *SI Appendix*. Thirty six hours after transfection, cells were rinsed with PBS and scraped into ice-cold lysis buffer (50 mM Tris-HCl [pH 7.4], 150 mM sodium chloride, 1% NP-40, 0.1% SDS, 1mM PMSF; 1mM N-ethylmaleimide, complete protease inhibitor cocktail all from Sigma). Lysates were rotated for 20min at 4°C and then centrifuged at 4°C at 13,000 x g for 5 min. For cycloheximide chase, cells were treated with 20  $\mu$ g/ml of cycloheximide for 7h prior to lysis without obvious cell death. For DUB activity measurements, cells were lysed in buffer (50 mM Tris-HCl [pH 7.4], 5 mM magnesium chloride, 250 mM sucrose, 1mM DTT; 2mM ATP) and equal amount of total protein was incubated with HA-Ubiquitin-Br2 as described previously (29).

**Design and construction of Usp8 or scrambled shRNA lentiviral vectors:**

The rat Usp8 sequence (accession no. NM\_001106502.1) was used to generate the Usp8 shRNA (5'CCGCTCGAGAAAAAGCTGAGATCTCAAGG

CTTTCTTGACAGGAAGA GAAAGCCTTGAGATCTCAGCCAAAAC  
AAGGCTTTTCTCCAAGG 3') which was predicted to knockdown the human  
protein as well along with a scrambled shRNA (5' CCGCTCGAGAAAAAA  
GGCACATTAGGAACCATACATTGACAGGAAGATGTATGGTTCCTAATGTG  
CCCAAAACAAGGCTTTTCTCCAAGG 3'). Short hairpin expression cassette  
comprised a sense and an antisense (antisense specific to the target mRNA)  
strand spaced by a loop sequence, RNA polymerase III transcription  
termination signal and XhoI restriction site. A sequence coding for the mouse  
U6 promoter was inserted upstream of the antisense strand, with a SpeI site.  
A PCR-based method was used to generate double-stranded shRNA  
expression cassettes using the pSilencer 1.0-U6 expression vector (Life  
Technologies, Carlsbad, CA, USA) as a transcription template and reverse  
primer encoding the shRNA oligonucleotides. These were subcloned into the  
lentiviral backbone pRRLsincpt.U6.CMV.EGFP.wpre (43) pre-digested with  
SpeI and XhoI, generating the  
pRRLsincpt.U6.rUsp8shRNA.CMV.EGFP.wpre or  
pRRLsincpt.U6.scrambledshRNA.CMV.EGFP.wpre constructs. The  
constructs were tested for efficiency in human cell lines and found to be  
effective in reducing the content of Usp8.

**Generation of human iPSc-derived neurons:** Dopaminergic neurons were  
derived from healthy control iPS cell lines that were previously described (42).  
as detailed in the *SI Appendix*.

**Colocalization studies:** Four to eight week old iPSc-derived neurons were plated onto Matrigel (BD Biosciences, Oxford, UK) -coated glass coverslips and HEK cells plated onto poly-L-lysine-coated glass coverslips. For Usp8 colocalization with Rab proteins in HEK-293T cells, fluorescently tagged plasmids expressing Rabs were transfected. For the bi-fluorescence complementation assay in HEK-293T cells, cells were co-transfected with WT Usp8-VN and WT Syn-VC, and fluorescently tagged plasmids expressing Rabs. Cells were probed with rabbit anti-Usp8 polyclonal antibody (HPA004869, 1:3000, Sigma), mouse anti- $\alpha$ -synuclein monoclonal antibody (610787, 1:500, BD Biosciences), goat anti-TH polyclonal antibody (101853, 1:400, Abcam, Cambridge, UK), mouse anti-EEA1 monoclonal antibody (610457, 1:500, BD Biosciences), mouse anti-LBPA monoclonal antibody (6C4, 1:200, Echelon Biosciences, Utah, USA) and mouse anti-Rab11 monoclonal antibody (A-6, 1:200, Santa Cruz) in PBS and visualized with Alexa 305-, 488-, 546- or 568-conjugated goat or donkey anti-mouse, -rabbit or -goat secondary antibodies (1:500, Life Technologies). Confocal imaging is detailed in *SI Appendix*. To measure the fractional overlap of the Usp8 stain with that of other markers, we have reported the Manders' Colocalization Coefficient (MCC), which measures the fraction of one protein that colocalizes with another, poorly measured by Pearson's Correlation Coefficient (44). MCC values range from zero (uncorrelated distributions of two probes with one another) to one (perfect colocalization of two images). No primary antibody controls were included for background subtraction.

**Deubiquitination of ubiquitinated  $\alpha$ -synuclein *in vitro*:** Purified  $\alpha$ -synuclein was ubiquitinated by Nedd4 as described previously (7).  $\alpha$ -Synuclein was incubated with His-Nedd4, His-Ubch5b, His-E1 and ubiquitin in the presence ATP. After ubiquitination, His-tagged enzymes were removed by incubation with Ni-NTA agarose (Qiagen). The unbound ubiquitinated  $\alpha$ -synuclein fraction was used as substrate of *in vitro* deubiquitination reaction.

Ubiquitinated  $\alpha$ -synuclein was incubated with the indicated DUBs (50 nM) in 50 mM Tris and 2 mM DTT at 37°C for 90 minutes. Each sample was analyzed by SDS-PAGE and immunoblotting using anti- $\alpha$ -synuclein antibody (C20, 1:1000, Santa Cruz). The recombinant DUBs (OTUB1, OTUB2, JosD2, Usp2 core, Usp5, Usp7, Usp8 core) used in this study were previously characterized ~~extensively by one of us (29)~~, and their activity was confirmed again using the active site-directed probe HA-UB-Br2 as described ~~previously~~ (29).

***Drosophila* genetics:** The *UAS- $\alpha$ -synuclein* wild-type (8146) and A53T mutant (8148), *UAS-Usp8 RNAi* (38982), *UAS-Ataxin 3* (8150) with expanded polyQ were obtained from Bloomington *Drosophila* Stock Center. The *UAS-Vps28 RNAi* (31894) was obtained from VDRC. The GAL4 UAS expression system was used to overexpress these transgenes either in dopaminergic neurons at 25°C using the *ddc*-GAL4 driver (kindly provided by A. Lin and G. Miesenbock), or specifically in the eye using *GMR*-GAL4 (provided by I. Davis) at 29°C. The following genotypes were used: (1) *+/+*; *ddc*-GAL4/*+* (2) *+/+*; *ddc*-GAL4/*UAS-A53T  $\alpha$ -synuclein* (3) *UAS-Usp8 RNAi* */+*; *ddc*-GAL4/*+* (4) *UAS-Usp8 RNAi*/*+*; *ddc*-GAL4/*UAS-A53T  $\alpha$ -synuclein* (5) *GMR*-

GAL4/+; (6) *GMR-GAL4/+; UAS- $\alpha$ -synuclein* /+ (7) *GMR-GAL4/+; UAS-A53T*  
 *$\alpha$ -synuclein* /+ (8) *GMR-GAL4/UAS-Usp8 RNAi* ; +/+ (9) *UAS-Usp8 RNAi* /  
*GMR-GAL4; UAS- $\alpha$ -synuclein* /+; (10) *Usp8 RNAi* / *GMR-GAL4; UAS-A53T*  
 *$\alpha$ -synuclein* /+ (11) *MS1096-GAL4/Y* (12) *MS1096-GAL4/Y; UAS-Usp8 RNAi*  
 /+ (13) *UAS- $\alpha$ -synuclein* / *GMR-GAL4; UAS-Vps28 RNAi* /+ (14) *UAS-Ataxin*  
*3* /*GMR-GAL4; UAS-Usp8 RNAi* /+; (15) *GMR-GAL4 /UAS-Ataxin 3* ; +/+(16)  
*UAS-AMSH RNAi* ; *ddcGAL4/+* (17) *UAS-JOSD2 RNAi* ; *ddcGal4/+* (18)  
*GMR-GAL4/UAS-AMSH RNAi* ; +/+ (19) *GMR-GAL4/UAS-AMSH RNAi* ;  
*UAS-A53T  $\alpha$ -synuclein* /+ (20) *UAS-JOSD2 RNAi/+* ; *UAS-A53T  $\alpha$ -synuclein*  
 /*ddcGAL4* (21) *UAS-AMSH RNAi/+* ; *UAS-A53T  $\alpha$ -synuclein* /*ddcGAL4* (22)  
*GMR-GAL4/+* ; *UAS-Usp14 RNAi/+* (23) *GMR-GAL4/+* ; *UAS-Usp47 RNAi/+*  
 (24) *GMR-GAL4/+* ; *UAS-Usp14 RNAi/ UAS-A53T  $\alpha$ -synuclein* (25) *GMR-*  
*GAL4/+* ; *UAS-Usp47 RNAi/ UAS-A53T  $\alpha$ -synuclein*. The experiments were  
 repeated in two independently derived transgenic lines and carried out with  
 the experimenter blinded to the sample genotypes throughout the analysis.

**Scanning electron microscopy of the *Drosophila* eye:** Age-matched, male  
 flies were fixed in 70% ethanol. The flies were then dehydrated in 100%  
 ethanol, dried and mounted on SEM stubs. The samples were then sputter  
 coated with gold and imaged using a JEOL JSM 6390 scanning electron  
 microscope. Eyes were examined for abnormal bristle orientation, ommatidial  
 fusion or pitting and disorganization of the ommatidial array.

**Fractionation of *Drosophila* head lysates:** All steps were performed at 4°C.  
 For each genotype, 5 male adult heads were homogenised in lysis buffer

(150mM NaCl, 10mM Tris pH 7.4 with complete protease inhibitor cocktail and 1mM N-ethylmaleimide). Crude lysates were centrifuged at 4,000g for 5min. Supernatants were then centrifuged at 100,000g for 1h. The resulting supernatant was designated as the cytosolic fraction whereas the pellet was resuspended in loading buffer.

**Climbing assays:** Locomotor function was assayed using a startle-induced negative geotaxis assay. Ten male flies were placed per vial and five vials were used per line in each experiment (total 50 flies per line). Each vial was tapped 10 times and the percentage of flies above 6cm was recorded after 4 sec.

**Quantitative RT-PCR.** Five fly heads from each line were homogenized for 30sec using a tissue homogenizer as detailed in the *SI Appendix*.

**Confocal Imaging of fly brains:** Fly brains were dissected at 25 days post-eclosion in ice-cold Schneider's fly medium and fixed in 4% PFA. They were washed in PBS-T, blocked in goat serum for 1h and then incubated for 48h at 4°C with monoclonal mouse anti-TH (1:500) followed by PBS-T washes and Alexa 488-coupled goat anti-mouse IgG (1:1000) for further 48h at 4°C. Stained brains were mounted in ProLong® Gold antifade mountant. Z-stacks of the brain were obtained on Zeiss LSM 780 confocal microscope using the 25x objective (1.4x digital zoom) at 1µm steps and z-projected. Dopaminergic neuronal clusters were identified and counted.

**Statistical analysis:** The statistical analysis was performed using the JMP software (SAS, version 10.0) and Prism (GraphPad). Outliers were identified using an outlier box plot and were excluded from the calculations where observed. All data was examined for distribution and statistical tests were chosen accordingly. For normal distributed data a *t*-test or a one-way ANOVA was used. For nonparametric data the Wilcoxon-Mann-Whitney and the Kruskal-Wallis test rank sum test were performed to assess differences in the mRNA or protein levels and for climbing assays. The null hypothesis was rejected at a significance level of  $p=0.05$ . Exponential data was log converted if reasonable before statistical calculation was performed. Correlations were estimated with a pairwise correlation method for normally distributed data and with Spearman's rho for nonparametric data. Colocalization was estimated as fractional overlap of two markers using the Manders' Colocalization Coefficient.

**Acknowledgements** We thank S. Cowley for providing the control iPS cell lines, M.G. Spillantini for the  $\alpha$ -synuclein cDNA, L. Parkkinen for assistance with the selection of neuropathological cases, D. Selkoe for the 2F12 antibody, F. Rinaldi for the lentiviral backbone, Bloomington and VDRC as well as A. Lin, G. Miesenbock and I. Davis for *Drosophila* stocks. This work was supported by a Wellcome Trust Intermediate Clinical Fellowship, the Wellcome Beit award and the NIHR Oxford Biomedical Research Centre to G.K.T. The Oxford Brain Bank is supported by Alzheimer's Brain Bank UK, the Medical Research Council and the NIHR Oxford Biomedical Research Centre.

## References

1. Braak H, Del Tredici K, Rub U, de Vos RA, Jansen Steur EN, Braak E (2003) Staging of brain pathology related to sporadic Parkinson's disease. *Neurobiology of Aging* 24: 197-211.
2. Spillantini MG, Schmidt ML, Lee VM, Trojanowski JQ, Jakes R, Goedert M (1997) Alpha-synuclein in Lewy bodies. *Nature* 388: 839-840.
3. Schneider JA, Arvanitakis Z, Yu L, Boyle PA, Leurgans SE, Bennett DA (2012) Cognitive impairment, decline and fluctuations in older community-dwelling subjects with Lewy bodies. *Brain* 135: 3005-3014.
4. Ross OA, *et al.* (2008) Genomic investigation of alpha-synuclein multiplication and parkinsonism. *Annals of Neurology* 63: 743-750.
5. Wirdefeldt K, Bogdanovic N, Westerberg L, Payami H, Schalling M, Murdoch G (2001) Expression of alpha-synuclein in the human brain: relation to Lewy body disease. *Brain Research Molecular brain research* 92: 58-65.
6. Tofaris GK, Layfield R, Spillantini MG (2001) alpha-Synuclein metabolism and aggregation is linked to ubiquitin-independent degradation by the proteasome. *FEBS Letters* 509: 22-26.
7. Tofaris GK, Kim HT, Hourez R, Jung JW, Kim KP, Goldberg AL (2011) Ubiquitin ligase Nedd4 promotes alpha-synuclein degradation by the endosomal-lysosomal pathway. *Proceedings of the National Academy of Sciences of the United States of America* 108: 17004-17009.
8. Kuzuhara S, Mori H, Izumiyama N, Yoshimura M, Ihara Y (1988) Lewy bodies are ubiquitinated. A light and electron microscopic immunocytochemical study. *Acta Neuropathologica* 75: 345-353.
9. Lowe J, *et al.* (1988) Ubiquitin is a common factor in intermediate filament inclusion bodies of diverse type in man, including those of Parkinson's disease, Pick's disease, and Alzheimer's disease, as well as Rosenthal fibres in cerebellar astrocytomas, cytoplasmic bodies in muscle, and Mallory bodies in alcoholic liver disease. *The Journal of Pathology* 155: 9-15.
10. Tofaris GK, Razzaq A, Ghetti B, Lilley KS, Spillantini MG (2003) Ubiquitination of alpha-synuclein in Lewy bodies is a pathological event not associated with impairment of proteasome function. *The Journal of Biological Chemistry* 278: 44405-44411.



11. Anderson JP, *et al.* (2006) Phosphorylation of Ser-129 is the dominant pathological modification of alpha-synuclein in familial and sporadic Lewy body disease. *The Journal of Biological Chemistry* 281: 29739-29752.
12. Schmidt M, Finley D (2014) Regulation of proteasome activity in health and disease. *Biochimica et Biophysica Acta* 1843: 13-25.
13. Nathan JA, Kim HT, Ting L, Gygi SP, Goldberg AL (2013) Why do cellular proteins linked to K63-polyubiquitin chains not associate with proteasomes? *The EMBO Journal* 32: 552-565.
14. Wollert T, Hurley JH (2010) Molecular mechanism of multivesicular body biogenesis by ESCRT complexes. *Nature* 464: 864-869.
15. Urbe S, McCullough J, Row P, Prior IA, Welchman R, Clague MJ (2006) Control of growth factor receptor dynamics by reversible ubiquitination. *Biochemical Society Transactions* 34: 754-756.
16. Mizuno E, Iura T, Mukai A, Yoshimori T, Kitamura N, Komada M (2005) Regulation of epidermal growth factor receptor down-regulation by UBPY-mediated deubiquitination at endosomes. *Molecular Biology of the Cell* 16: 5163-5174.
17. Mukai A, Yamamoto-Hino M, Awano W, Watanabe W, Komada M, Goto S (2010) Balanced ubiquitylation and deubiquitylation of Frizzled regulate cellular responsiveness to Wg/Wnt. *The EMBO Journal* 29: 2114-2125.
18. Reincke M *et al.*, Mutations in the deubiquitinase gene USP8 cause Cushing's disease. *Nature Genetics* 47:31-38.
19. Ma ZY *et al.* (2015) Recurrent gain of function USP8 mutations in Cushing's disease. *Cell Research* 25: 306-317.
20. Kirkin V, *et al.* (2009) A role for NBR1 in autophagosomal degradation of ubiquitinated substrates. *Molecular Cell* 33: 505-516.
21. Row PE, Liu H., Hayes S, Welchman P, Charalambous K, Hofmann K, Clague MJ, Sanderson S, Urbe S (2007) The MIT domain of UBPY constitutes a CHMP binding and endosomal localisation signal required for efficient epidermal growth factor receptor degradation. *The Journal of Biological Chemistry* 282: 30929-30937.
22. Ali N, Zhang L, Taylor S, Mironov A, Urbe S, Woodman P (2013) Recruitment of UBPY and ESCRT exchange drive HD-PTP-dependent sorting of EGFR to the MVB. *Current biology* 23: 453-461.
23. Chen L, Periquet M, Wang X, Negro A, McLean PJ, Hyman BT LM, Feany MB (2009) Tyrosine and serine phosphorylation of alpha-synuclein have

opposing effects on neurotoxicity and soluble oligomer formation. *Journal of Clinical Investigation* 119: 3257-32659.

24. Davies SE, *et al.* (2014) Enhanced ubiquitin-dependent degradation by Nedd4 protects against alpha-synuclein accumulation and toxicity in animal models of Parkinson's disease. *Neurobiology of Disease* 64: 79-87.
25. Auluck PK, Chan HY, Trojanowski JQ, Lee VM, Bonini NM (2002) Chaperone suppression of alpha-synuclein toxicity in a *Drosophila* model for Parkinson's disease. *Science* 295: 865-868.
26. Lu L, *et al.* (2005) Gene expression profiling of Lewy body-bearing neurons in Parkinson's disease. *Experimental Neurology* 195: 27-39.
27. Hasegawa M, *et al.* (2002) Phosphorylated alpha-synuclein is ubiquitinated in alpha-synucleinopathy lesions. *The Journal of Biological Chemistry* 277: 49071-49076.
28. Ritorto M, *et al.* (2014) Screening of DUB activity and specificity by MALDI-TOF mass spectrometry. *Nature Communications* 5: 4763
29. McGouran JF, Gaertner SR, Altun M, Kramer HB, Kessler BM (2013) Deubiquitinating enzyme specificity for ubiquitin chain topology profiled by di-ubiquitin activity probes. *Chem Biol.* 20:1447-1455.
30. Swaminathan S, Amerik AY, Hochstrasser M (1999) The Doa4 deubiquitinating enzyme is required for ubiquitin homeostasis in yeast. *Molecular Biology of the Cell* 10: 2583-2594.
31. Dupre S, Haguenaue-Tsapis R (2001) Deubiquitination step in the endocytic pathway of yeast plasma membrane proteins: crucial role of Doa4p ubiquitin isopeptidase. *Molecular and Cellular Biology* 21: 4482-4494.
32. Sugeno N, *et al.* (2014) Lys-63-linked ubiquitination by E3 ubiquitin ligase Nedd4-1 facilitates endosomal sequestration of internalized alpha-synuclein. *The Journal of Biological Chemistry* 289: 18137-18151.
33. Wijayanti I, Watanabe D, Oshiro S, Takagi H (2015) Isolation and functional analysis of yeast ubiquitin ligase Rsp5 variants that alleviate the toxicity of human  $\alpha$ -synuclein. *Journal of Biochemistry* 157: 251-260
34. Boassa D, *et al.* (2013) Mapping the subcellular distribution of alpha-synuclein in neurons using genetically encoded probes for correlated light and electron microscopy: implications for Parkinson's disease pathogenesis. *The Journal of Neuroscience* 33: 2605-2615.
35. Hasegawa T, *et al.* (2011) The AAA-ATPase VPS4 regulates extracellular secretion and lysosomal targeting of alpha-synuclein. *PloS One* 6: e29460.

36. Scudder SL, *et al.* (2014) Synaptic strength is bidirectionally controlled by opposing activity-dependent regulation of Nedd4-1 and Usp8. *The Journal of Neuroscience* 34: 16637-16649.
37. Perrett RM, Alexopoulou Z, Tofaris GK (2015) The endosomal pathway in Parkinson's disease. *Molecular Cellular Neuroscience* doi: 10.1016/j.mcn.2015.02.009.
38. Lu K *et al.* (2014) Autophagic clearance of polyQ proteins mediated by ubiquitin-Atg8 adaptors of the conserved CUET protein family. *Cell* 158: 549-63.
39. Tofaris GK (2012) Lysosome-dependent pathways as a unifying theme in Parkinson's disease. *Movement Disorders* 27: 1364-1369.
40. Bruzzone F *et al.* (2008) Expression of the deubiquitinating enzyme mUBPy in the mouse brain. *Brain Res* 1195:56-66.
41. McKeith IG *et al.* (2005) Diagnosis and management of dementia with Lewy bodies: third report of the DLB Consortium. *Neurology* 65: 1863-1872.
42. Hartfield EM, *et al.* (2014) Physiological characterisation of human iPS-derived dopaminergic neurons. *PloS One* 9: e87388.
43. Rinaldi F, *et al.*, (2014) Cross-regulation of Connexin43 and beta-catenin influences differentiation of human neural progenitor cells. *Cell Death Dis* 5: p. e1017.
44. Dunn KW, Kamocka MM, McDonald JH (2011) A practical guide to evaluating colocalization in biological microscopy. *American Journal of Physiology Cell Physiology* 300: 723-742.

## Figures

**Fig. 1: K63-linked ubiquitin conjugates are detected in  $\alpha$ -synuclein positive inclusions and are reduced in the substantia nigra. (A)**

Schematic view of studied brain regions and corresponding light microscopy images showing K63-linked ubiquitinated inclusions. Bar schemes 5mm, bar images 20mm. (B) Confocal immunofluorescence showing colocalization of K63-linked ubiquitin chains and  $\alpha$ -synuclein in Lewy bodies and Lewy neurites

in nigral neurons. (C) Quantification of ubiquitin-positive inclusions as a percent of  $\alpha$ -synuclein positive inclusions (Ub/ $\alpha$ -Syn) in serial sections of the AC, EC and SN,  $p < 0.0001^*$ ,  $n = 14$ . (D) Quantification of K63-linked ubiquitinated inclusions as a percent of  $\alpha$ -synuclein positive inclusions (K63-Ub/ $\alpha$ -Syn) in serial sections of AC, EC and SN,  $p < 0.0001^*$ ,  $n = 14$ . (E) The percentage of ubiquitinated inclusions in nigral neurons was low irrespective of the stage of disease and higher in incidental Lewy Body (ILB) compared to Lewy Body Disease (LBD) cases. Ub/Syn  $p < 0.0001^*$ ,  $n = 14$ , K63/Syn  $p < 0.05^*$ ,  $n = 14$ . Abbreviations: anterior cingulate (**AC**), corpus callosum (CC), lateral ventricle (LAT.V.); entorhinal cortex (**EC**), cornu ammonis 1-4 (CA1-4), dentate gyrus (DG); substantia nigra (**SN**), central aqueduct (AQ), inferior colliculus (IC), corticopontine and pyramidal tracts (CP).

**Fig. 2: Usp8 expression and localization inversely correlates with ubiquitinated inclusions in  $\alpha$ -synucleinopathies.** (A) Representative immunoblot showing increased levels of Usp8 but not AMSH relative to the actin loading control in the SN from patients with LB disease; specific band shown by arrowhead. (B) Quantification of Usp8 protein level in the human brain showed a significant increase in the SN but not AC of patients with Lewy body disease when compared to controls ( $p = 0.0028^*$ ,  $n = 8$ ). (C) Quantification of AMSH protein levels did not show a significant difference. Usp8 positive LB and LN in the AC (panel D) and SN (panel E), bar 20 $\mu$ m. (F) No AMSH staining was seen in nigral LB, indicated with arrowhead. (G) Double immunofluorescence and confocal imaging confirmed the colocalization of Usp8 (red) and  $\alpha$ -synuclein (green) in nigral LB. DAPI indicates nuclear

staining in blue. (H) Quantification of Usp8-positive as a percent of  $\alpha$ -synuclein-positive inclusions (Usp8/ $\alpha$ -Syn) in serial sections showed a significant increase in the SN compared to cortical areas (AC, EC) ( $p=0.0001^*$ ,  $n=14$ ). (I) Negative correlation between Usp8-positive and ubiquitin-positive inclusions in the SN ( $p=0.0002^*$ ,  $\rho=-0.5044$ ). (J) Negative correlation of Usp8-positive and Lys63-linked ubiquitinated inclusions shown as ratio of K63/Ub ( $p=0.0038^*$ ,  $\rho=-0.4186$ ).

**Fig. 3: Usp8 interaction and co-localisation with  $\alpha$ -synuclein.** (A) Wild-type (Usp8<sup>WT</sup>) or catalytically inactive (Cys786 to Ala, Usp8<sup>CA</sup>) Usp8 was immunoprecipitated with untagged  $\alpha$ -synuclein when expressed in HEK-293T cells. (B) Usp8 activity as measured by binding to HA-Ub-Br2 is not affected by increasing  $\alpha$ -synuclein levels or expression of  $\alpha$ -synuclein mutants (C). Bimolecular fluorescence complementation signifying Usp8/ $\alpha$ -synuclein interaction and expression of endosomal Rabs (Rab5, Rab7, Rab11) tagged to a Red fluorescent protein. Schematic depicting the bimolecular fluorescence complementation assay utilized in this study. Human Usp8 is tagged to the N-terminus fragment of Venus fluorescent protein (VFP) and  $\alpha$ -synuclein to the C-terminus fragment of VFP. Quantification of the percentage overlap (Manders' Colocalization Coefficient, MCC) between Usp8/ $\alpha$ -synuclein (green) with the indicated endosomal markers (red);  $n=100$  cells per condition;  $p<0.001$ ; One way ANOVA. (D) Localisation of Usp8 in relation to endosomal markers in human iPSc-derived dopaminergic neurons: Triple labeling of neurons with TH (for detection of dopaminergic neurons, first column, blue), Usp8 (second column green) and one of the following: (i) early

endosome, EEA1, (ii) late endosome, LBPA or (iii)  $\alpha$ -synuclein (third column, red). Quantification of the percentage overlap (Manders' Colocalization Coefficient, MCC) of Usp8 with the indicated markers in panel **b**; n=50 neurons per condition.

**Fig. 4: Usp8 de-conjugates preferentially K63-linked ubiquitin chains on**

**$\alpha$ -synuclein.** (A) Expression of Usp8<sup>WT</sup> caused robust deubiquitination of endogenous  $\alpha$ -synuclein when compared to expression of Usp8<sup>CA</sup> or empty vector. Quantification of ubiquitinated  $\alpha$ -synuclein in Usp8<sup>WT</sup> relative to Usp8<sup>CA</sup> expressing cells shown as arbitrary units (AU, p=0.0410\*, n=3 biological replicates). (B) Co-expression of Usp8 with either K63 or K48 single lysine ubiquitin showed that it de-conjugated preferentially K63-linked chains on  $\alpha$ -synuclein without any obvious difference in total amount of ubiquitinated proteins between the immunoprecipitated samples (representative of n=3 biological replicates). (C) Expression of a deletion mutant of Usp8 lacking the MIT domain required for endosomal localization, (Usp8 <sup>$\Delta$ MIT</sup>) reduced its activity against K63-linked ubiquitin chains on  $\alpha$ -synuclein when compared to Usp8<sup>WT</sup>. Usp7 had reduced activity against  $\alpha$ -synuclein when compared to Usp8 in cells (n=5 biological replicates). (D) Recombinant  $\alpha$ -synuclein was linked to uniform K63-linked chains *in vitro* by purified Nedd4 and incubated with the indicated deubiquitinases (50nM). Robust deubiquitination was observed with Usp7 and Usp8. All seven enzymes were assessed for purity with Coomassie and activity by HA-Ub-br labeling. Immunoblotting with anti-

HA revealed a shift in the molecular weight of labeled DUBs, which indicates covalent binding to HA-Ub-br.

**Fig. 5: Usp8 regulates the degradation of  $\alpha$ -synuclein by the lysosome.**

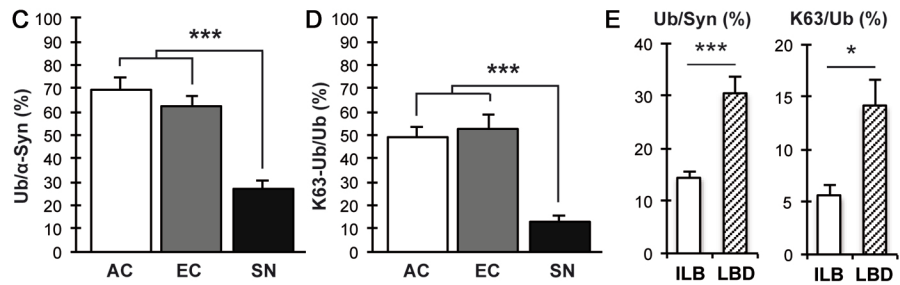
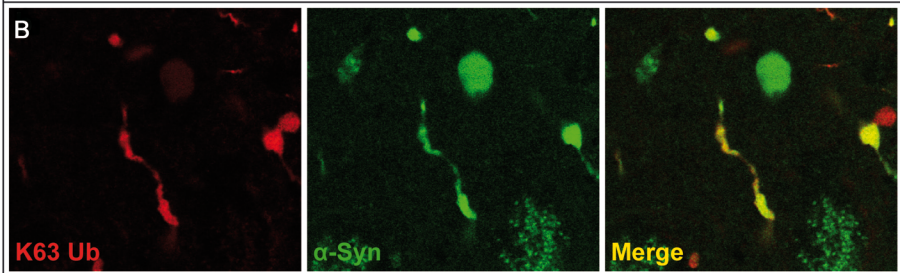
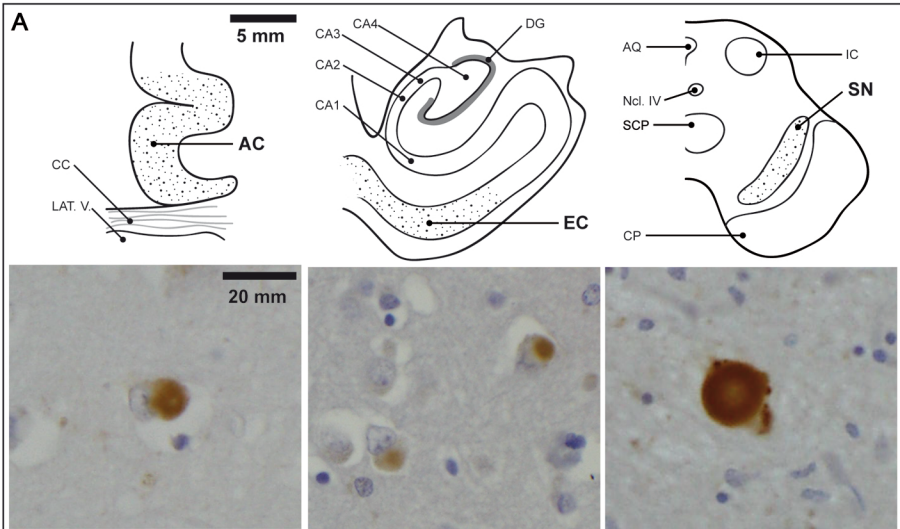
(A) Cycloheximide chase of endogenous  $\alpha$ -synuclein showed that its rate of clearance was reduced at 7h when wild-type Usp8 was expressed in HEK-293T cells, ( $p=0.0091^{**}$ ,  $n=3$  biological replicates). (B) Lentiviral mediated shRNA knockdown of Usp8 in SH-SY5Y cells reduced endogenous  $\alpha$ -synuclein levels by 35% relative to actin loading control when compared to scr shRNA controls ( $p=0.0031^{**}$ ,  $n=5$  biological replicates) and (C) increased the amount of ubiquitinated  $\alpha$ -synuclein as evidenced by immunoblotting of immunoprecipitated  $\alpha$ -synuclein with anti-ubiquitin and anti-K63 antibodies. (D) Membrane fractions enriched in endosomal/autophagic lysosomal compartments were isolated from Usp8 knockdown and Scr shRNA control SH-SY5Y cells and tested for  $\alpha$ -synuclein levels at baseline and following 8h of treatment with either 50 $\mu$ M chloroquine (CQ) or 5 $\mu$ M lactacystin (Lact). Accumulation of  $\alpha$ -synuclein was observed in Usp8 knockdown cells treated with chloroquine suggesting that there is accelerated lysosomal degradation of  $\alpha$ -synuclein in these cells ( $p=0.019$ ,  $n=3$ ).

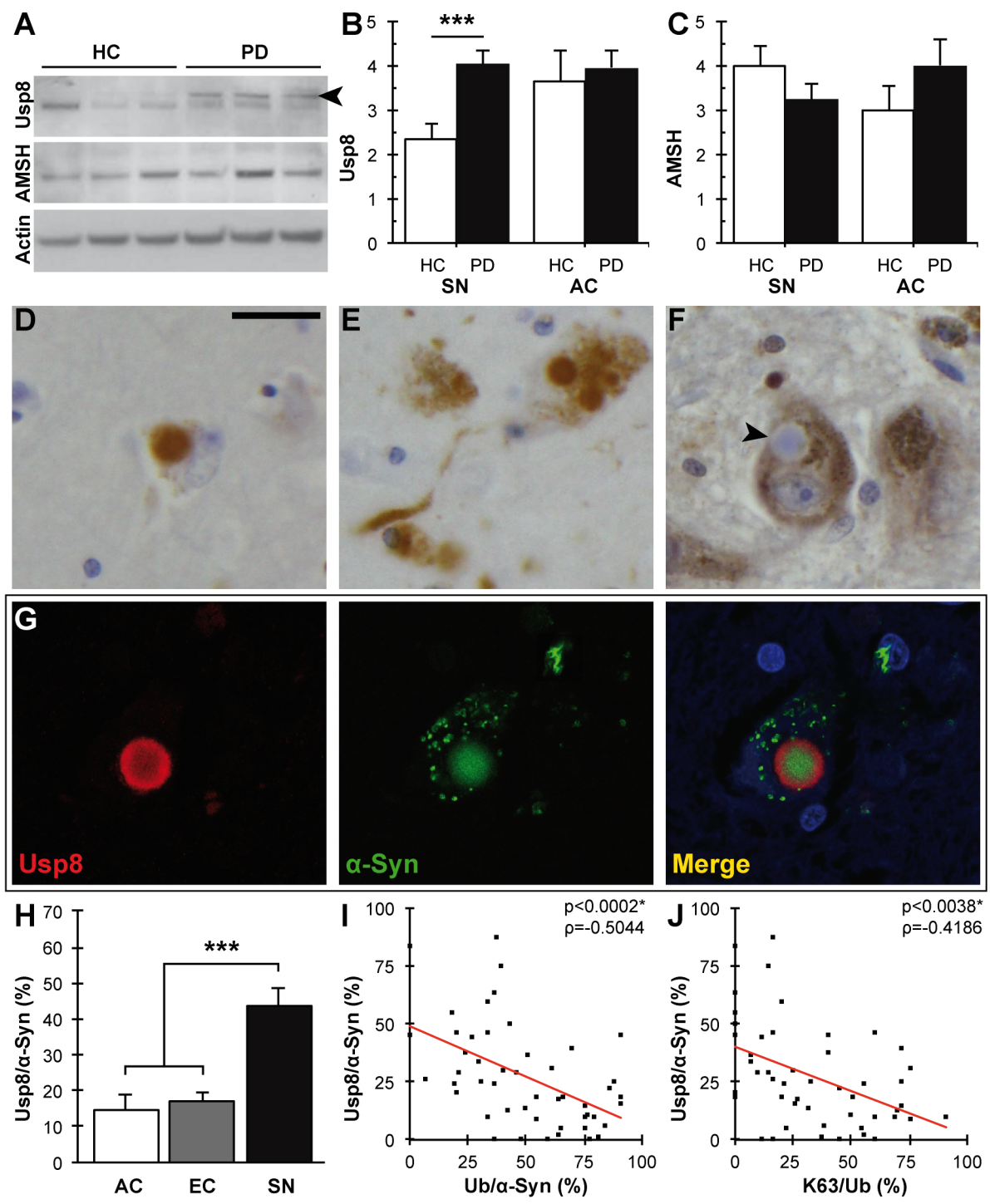
**Fig. 6: Knockdown of endogenous Usp8 in *Drosophila* protects against  $\alpha$ -synuclein-induced toxicity.** Overexpression of  $\alpha$ -synuclein caused a rough eye phenotype, which was more severe in flies expressing the A53T mutant  $\alpha$ -synuclein as detected by SEM. This phenotype was rescued in double transgenic flies with eye specific Usp8 knockdown and either wild-type

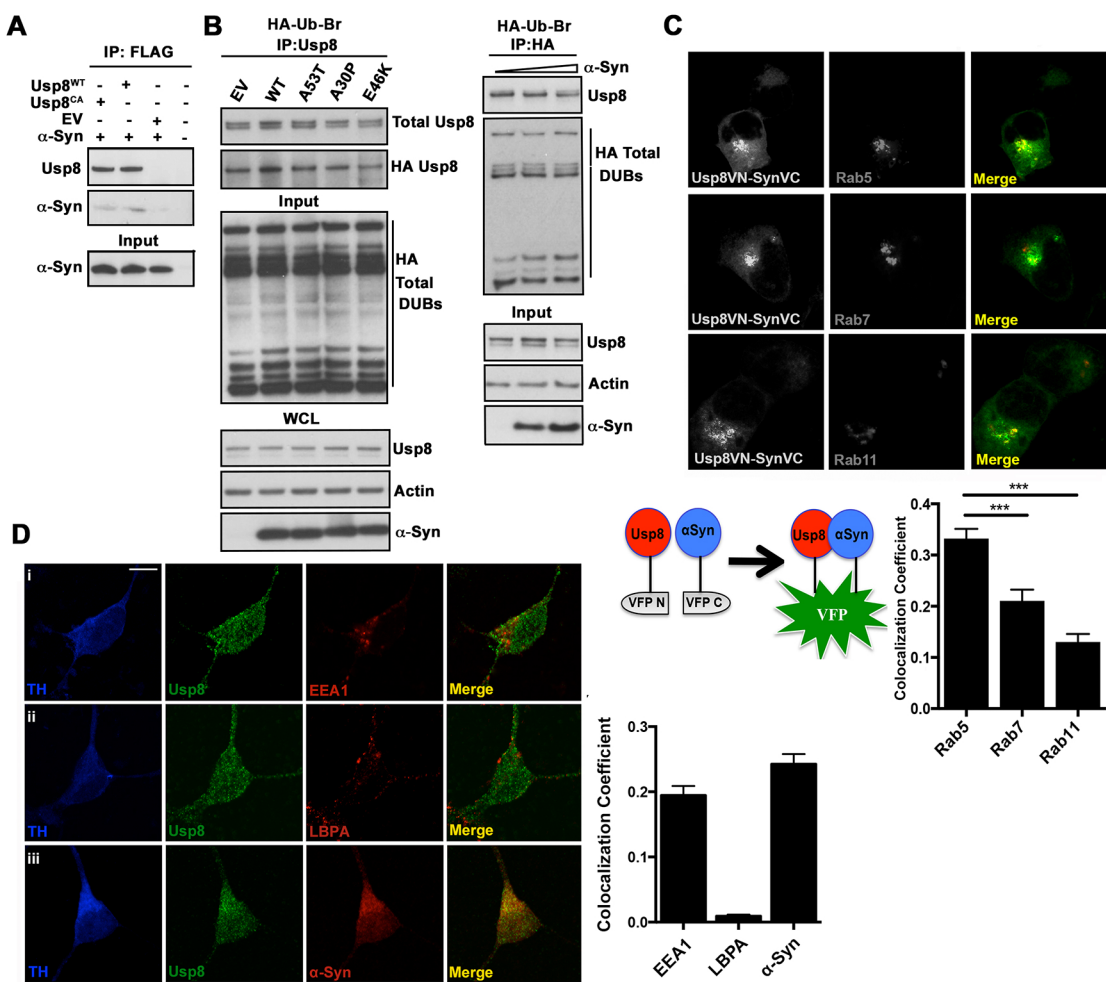
(panel *A*) or A53T mutant  $\alpha$ -synuclein (panel *B*). Quantitative PCR did not show a reduction in  $\alpha$ -synuclein mRNA levels between single and double transgenic lines to explain the phenotype. (*C*) Knockdown of AMSH did not rescue this phenotype whereas knockdown of Vps28 made it worse. (*D*) Usp8 knockdown did not affect the expanded Ataxin 3 phenotype. (*E*) Representative immunoblot of fractionated lysate (C=Cytosol, P=Pellet) from A53T mutant  $\alpha$ -synuclein flies and flies expressing A53T mutant  $\alpha$ -synuclein with Usp8 knockdown (labelled +Usp8 KD). Quantitative band densitometry showed that, relative to actin loading control, protein levels of either wildtype or A53T mutant monomeric  $\alpha$ -synuclein (indicated by \*) were significantly reduced in flies co-expressing Usp8 RNAi (n=4 biological replicates) in the absence of a reduction in mRNA levels as shown panels *A*, *B*. (*F*) Accelerated loss of climbing ability was seen in transgenic flies expressing human A53T mutant  $\alpha$ -synuclein in dopaminergic neurons (*ddc*-GAL4 driver) with increasing age. The climbing ability of double transgenic lines expressing A53T  $\alpha$ -synuclein with Usp8 knockdown in dopaminergic cells was significantly improved (shown by asterisks) when compared to A53T  $\alpha$ -synuclein expressing flies and was similar to the control genotype, *ddc*-GAL4/+ (p=0.0381\* for day 10; p=0.01\*\* for day 12; p=0.0159\* for day 14; n=50 flies per group). (*G*) Knockdown of JosD2 or AMSH in dopaminergic neurons slightly worsened the A53T mutant  $\alpha$ -synuclein phenotype. (*H*) Expression of A53T mutant  $\alpha$ -synuclein but not control constructs in dopaminergic neurons (*ddc*-GAL4 driver) led to loss of TH-immunoreactive neurons in the PPM1/2 cluster which was prevented by concomitant Usp8 knockdown (p<0.01\*\*).

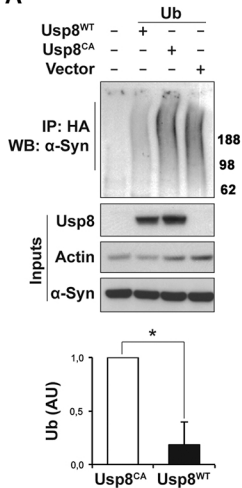
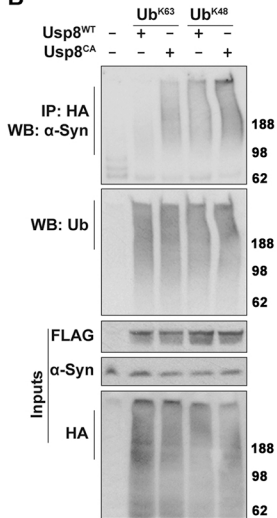
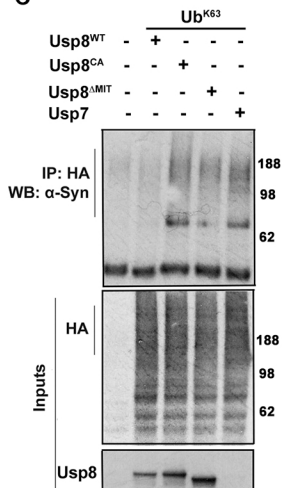
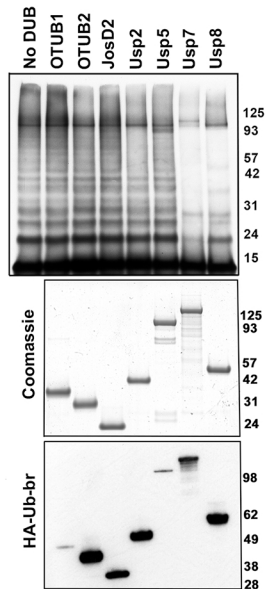


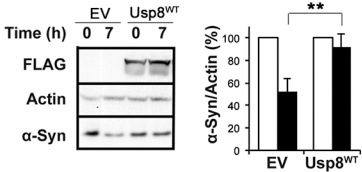
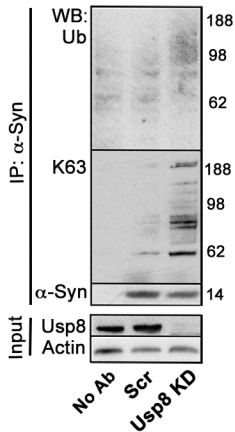
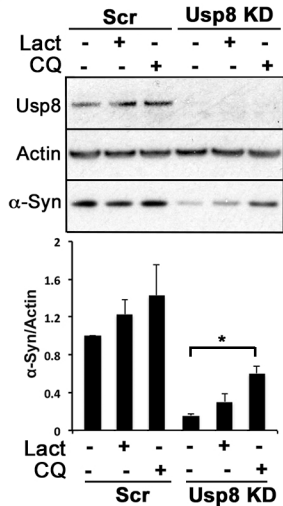
**Supplementary Table 1 and Figures 1-8 are included in the SI Appendix**







**A****B****C****D**

**A****C****D****B**